Energy and Buildings 133 (2016) 853–866

Contents lists available at ScienceDirect

Energy and Buildings

journal homepage: www.elsevier.com/locate/enbuild

Residential building design optimisation using sensitivity analysis and genetic algorithm

Facundo Bre[a,b,*], Arthur Santos Silva[c], Enedir Ghisi[c], Víctor D. Fachinotti[a]

[a] Centro de Investigación de Métodos Computacionales (CIMEC), UNL, CONICET, Predio "Dr. Alberto Cassano", Colectora Ruta Nacional 168 s/n, 3000 Santa Fe, Argentina

[b] Grupo de Investigación en Mecánica Computacional y Estructuras (GIMCE), Facultad Regional Concepción del Uruguay (FRCU), Universidad Tecnológica Nacional (UTN), 3260 Concepción del Uruguay, Argentina

[c] Federal University of Santa Catarina, Department of Civil Engineering, Laboratory of Energy Efficiency in Buildings, Florianópolis 88040-900, SC, Brazil

ARTICLE INFO

Article history:
Received 30 June 2016
Received in revised form
22 September 2016
Accepted 19 October 2016
Available online 25 October 2016

Keywords:
Residential building
Multi-objective optimisation
Energy consumption
Hybrid ventilation
Sensitivity analysis
Genetic algorithms
EnergyPlus

ABSTRACT

The objective of this paper is to combine sensitivity analysis and simulation-based optimisation in order to optimise the thermal and energy performance of residential buildings in the Argentine Littoral region. An actual house was selected as case study. This is a typical, local, single-family house having some rooms conditioned only by natural ventilation, and other rooms with natural ventilation supplemented by mechanical air-conditioning (hybrid ventilation). Hence, the total degree-hours at the naturally ventilated living room and the total energy consumption by air-conditioning at the bedrooms were chosen as objective functions to be minimised. The global objective function characterising the thermal and energy performance of the house was defined as the weighted sum of these objective functions. This objective function was computed using the EnergyPlus building performance simulation programme. Then, we performed a sensitivity analysis using the Morris screening method to rank the influence of the design variables on the objective function. This showed that the type of external walls, the windows infiltration rate and the solar azimuth were the most influential design variables on the given objective function for the considered house, and also that the azimuth either had a highly nonlinear effect on the objective function or was highly correlated to the others variables, deserving in any case a finer discretisation.

Finally, we solved an optimisation problem using genetic algorithms in order to find the optimal set of design variables for the considered house. The results highlighted the efficiency and the effectiveness of the proposed methodology to redesign a typical house in the Argentine Littoral region, improving hugely its thermal and energy performance.

1. Introduction

Nowadays, buildings are the largest energy consumers in Argentina [1]: considering the total energy (mainly electricity and gas), 26% is consumed by residential buildings and 8% is consumed by public and commercial buildings. Furthermore, the supply, transport and distribution of electricity in Argentina is facing a critical situation (the current level of operational reserve under extreme meteorological conditions is less than 5% of the whole available power, the availability of the imported gas and diesel is uncertain in the medium term), leading the central government to declare the national electricity sector in state of emergency on December 2015 [2]. This urges to reduce the energy consumption in buildings, mainly in the residential ones.

In this work, we focus on residential buildings located in the Argentine Littoral region (from now on referred to as "Littoral"). This 0.5-million km^2 area is located in northeastern Argentina, southeastern South America, see Fig. 1. Its climate is Cfa according to the Köppen-Geiger classification [3]. In a finer classification [4], Littoral is divided into three bioclimatic zones (those ones separated by red dashed lines in Fig. 1: very hot in the north (I), hot in the centre (II), and warm temperate in the south (III). Further, each zone is divided into two subzones *a* and *b*, those ones separated by a green dashed line in Fig. 1, regarding the daily temperature range be greater or lesser than 14 °C. Temperatures throughout Littoral are already not only high to very high during summer, but also they will be 2–4.5 °C higher by 2100 according to the 2014 report of the Intergovernmental Panel on Climate Change (IPCC) [5]. Although we have no information to quantify the concomitant increase of cooling demand in Littoral, we refer to studies in the USA pointing

* Corresponding author at: Centro de Investigación de Métodos Computacionales (CIMEC), UNL, CONICET, Predio "Dr. Alberto Cassano", Colectora Ruta Nacional 168 s/n, 3000 Santa Fe, Argentina.
E-mail address: facubre@cimec.santafe-conicet.gov.ar (F. Bre).

http://dx.doi.org/10.1016/j.enbuild.2016.10.025
0378-7788/

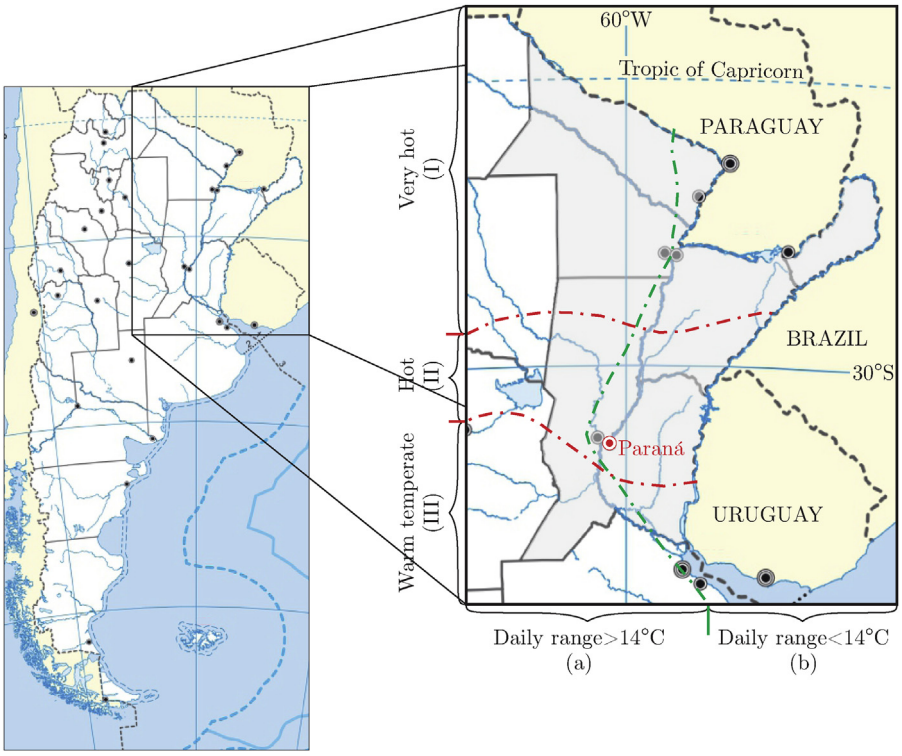

Fig. 1. Map of the Argentine Littoral Region (in light grey), showing the bioclimatic zones (I, II or III, a or b) and the location of the studied house (Paraná). (For interpretation of reference to color in this figure legend, the reader is referred to the web version of this article.)

out that the electricity demand for residential cooling will increase by roughly 5–20% per 1 °C warming [6]. Combined with the current state of emergency in the Argentine electricity sector, these estimates make the improvement of building energy efficiency even more urgent in Littoral.

For the architectural design of an energetically efficient building, the thermal and energy performance of a large series of alternative designs of such building must be analysed in seek of a sufficiently good or even optimal solution. Building performance simulation (BPS) makes affordable the study of a large number of alternative designs, allowing the designer to achieve specific objectives such as reducing environmental impact and energy consumption or improving the indoor thermal comfort [7]. The most popular software for BPS, EnergyPlus [8], is used in this work.

Since a time ago, researchers had been making significant efforts to automate the search of more efficient designs. A pioneer in this area is Wright [9], who applied the direct search method to optimise HVAC systems. Since that time, different objectives, design variables, and optimisation algorithms have been considered: Fesanghary et al. [10] used a harmony search algorithm to minimise the life cycle cost and carbon dioxide equivalent emissions of residential buildings; Bichiou and Krarti [11] optimised the building envelope and the HVAC design and operation using three different methods (genetic algorithm, particle swarm algorithm and sequential search), comparing them in terms of robustness and effectiveness; Ihm and Krarti [12] applied a sequential search method to optimise the design of residential buildings in Tunisia; Nguyen and Reiter [13] used a particle swarm optimisation and hybrid algorithms to optimise passive designs and strategies for low-cost housing. Recent reviews of the optimisation methods applied to building energy performance are given by Evins [14], Nguyen et al. [15], and Machairas et al. [16]. From these reviews, it is concluded that genetic algorithms (GA) are the widest used methods in building design optimisation, the reasons being that they do not "get stuck" in local optima, they have low sensitivity to discontinuities in the objective function, and they are well-suited for parallel computing. Considering these advantages, we choose GA as the current optimisation method.

Some authors used the sensitivity analysis (or "design of experiment" method) as an alternative to mathematical optimisation to improve the building performance [17–19]. Primarily, sensitivity analysis gives a ranking of the influence of the design variables on the objective. In this work, we decided to use this method not to improve the building performance but to determine the relevant design variables. Subsequently, we kept only such variables for the optimisation problem, making it cheaper to solve. Up to our knowledge, the only previous work combining sensitivity analysis and optimisation for building energy performance was performed by Evins et al. [20]. In their study, the objective was computed on the base of building regulations, which is a crucial difference with the current approach where the energy performance of the building is computed using EnergyPlus (the objective being defined by such performance). Further, we used the Morris screening method [21] for sensitivity analysis, which is considerably cheaper than the factorial method used by Evins et al. [20] from the computational point of view.

In summary, this paper presents a methodology for the optimisation of thermal and energy performance of a house, combining: (1) EnergyPlus to evaluate such performance; (2) sensitivity analysis to keep as design variables only the relevant ones; and (3) genetic algorithms as optimisation solver. Finally, we show that the application of such methodology for the design of a typical house in Littoral makes affordable a huge improvement of the thermal and energy performance of this house.

2. Case study

Let us take as case study a typical residential building in Littoral, particularly at Paraná, a city located in the centre of Littoral, with latitude 31.78S, longitude 60.48W and altitude 78 m. We have

Fig. 2. *Roble2D* single-family house.

Table 1
Characteristics of the *Roble2D* single-family house.

Element	Characteristics
Building azimuth	0 (i.e., façade facing North)
Type of external walls	Hollow brickwork layer with mortar finish
External solar absorptance of external walls	0.7
Type of windows	Simple clear 3 mm-thick glass
Shading fraction in windows	25%
Infiltration rate in windows and doors	0.02 kg/(sm)
Window area fraction for natural ventilation	30%
Type of roof	Ceramic tile, air gap and concrete liner
Type of internal walls	Hollow brickwork layer with mortar finish
Type of the first floor	Concrete with ceramic floor

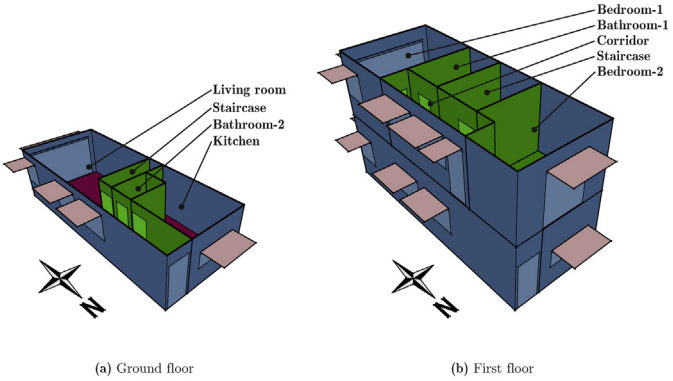

Fig. 3. Thermal zones of the building simulation model.

recently defined the typical meteorological year (TMY) at Paraná [22], to be used in this work.

In Argentina, the building codes do not define a reference or standard house for energy efficiency. So, we adopted as a typical house in Littoral one of the house models funded by the credit programme PROCREAR [23]), supported by the Argentine national government. This programme was launched in June 2012 and aimed to fund 400,000 single-family homes; half of them had already been finished by November 2015. The model for this study is the so-called *Roble2D* (2D stands for two bedrooms) depicted in Fig. 2. This is a 83 m^2 two-story, detached house composed of one kitchen, one living room and one bathroom on the ground floor, and two bedrooms, a corridor, and a bathroom on the first floor.

Further characteristics of this house are shown in Table 1.

3. Building model

The house was modelled using EnergyPlus version 8.4.0 [8,24], from now on referred to as E^+. This is an energy simulation programme addressed to model heat transfer and energy consumption in buildings for heating, cooling, ventilation, lighting and other needs. Some of the main capabilities of E^+ are: (1) integrated and simultaneous solution of thermal zone conditions and HVAC systems; (2) heat balance-based solution of radiant and convective effects on thermal comfort; (3) interaction between thermal zones and the environment is accounted for each short time step (even a fraction of an hour); and (4) heat and mass transfer are coupled to account for air movement between zones.

For analysis with E^+, we considered each room and the staircase as individual thermal zones, yielding the eight zones depicted in Fig. 3. All the zones were modelled as *FullExterior* E^+ objects [25], which allowed us to take into account the effect of shadows on their external surfaces. The windows and shadowing devices were assumed to have parametrically adjustable dimensions to facilitate the sensitivity and optimisation study later on. In order to simplify the model, the three windows in the corridor as well as the three ones on Surface-4 in the living room (see Fig. 4) were replaced with equivalent windows, one per each case. Each equivalent window has a fixed height and a variable width.

Since the heat transfer with the ground is a significant load component in low-rise buildings [26], we considered a volume of the ground around the house, modelled as an E^+ *GroundDomain:Slab*

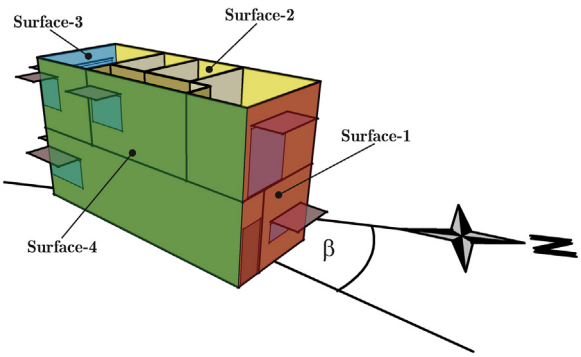

Fig. 4. External surfaces of the house. The azimuth angle β is the angle between the true North and the vector normal to Surface-1, measured in clockwise direction.

object. The outdoor portion of the ground surface is assumed to be exposed to the weather, represented by the local daily average of global horizontal radiation, air temperature, relative humidity, and wind speed computed from the local TMY file, as proposed by Xing [27]. Heat flows naturally from the house and the ground through the indoor portion of the ground surface, evolving all along the year according to the weather and the thermal response of the house.

The rooms cooled by natural ventilation (all of them except the bedrooms) were modelled as *AirflowNetwork* E+ objects. We assumed the windows and doors to be temperature-controlled in order to allow airflow when the indoor temperature was higher than the outdoor and whenever the outdoor temperature was higher than 20 °C.

In each bedroom, whenever natural ventilation was not enough for ensuring the thermal comfort, the air-conditioner was turned on and the airflow was blocked. This was prescribed by using the *HybridVentilation Manager* E+ object. The air-conditioners in the bedrooms were modelled as packaged terminal heat pumps (PTHP). They were allowed to work for heating when the room temperature was less than or equal to 18 °C, and for cooling when the room temperature was greater than or equal to 26 °C, whenever the bedrooms were occupied (according to the schedule shown in Fig. 5). The air-conditioners were assumed to have a coefficient of performance (COP) equal to 3.0 and 2.75 for the cooling coil and the heat pump, respectively, and an efficiency of 0.70 for the fan, values that are recommended by the Brazilian regulations RTQ-R [28] and are given by default in E+ [25]. Let us notice that the Brazilian regulation applies to zones that are geographically and bio-climatically close to Littoral, being our best-possible choice in absence of local regulations.

3.1. Internal heat loads

The Roble2D house has been designed to be occupied by four people. We assumed each bedroom and the living room to be occupied by two and four people respectively, according to the schedules depicted in Fig. 5. These rooms were –by far– the most occupied ones and, because of this, the only rooms where internal loads were considered, as recommended by the Brazilian regulation RTQ-R [28].

As internal heat sources, we included the residents, the lighting, and the equipment. Each occupant was assumed to produce 108 W in the living room and 81 W in the bedrooms, following ASHRAE [29]. The bedrooms and the living room had surface-mounted fluorescent luminaries. We assumed the lights in the living room and the bedrooms to be turned on or off according to the corresponding schedules shown in Fig. 6(a) and (b). The lighting power density was 5 W/m^2 in the bedrooms and 6 W/m^2 in the living room. Further, the living room had electric equipment producing 1.5 W/m^2 all over the day. The radiant fraction was assumed to be 0.72 for luminaries and 0.50 for the equipment, as suggested by ASHRAE [29].

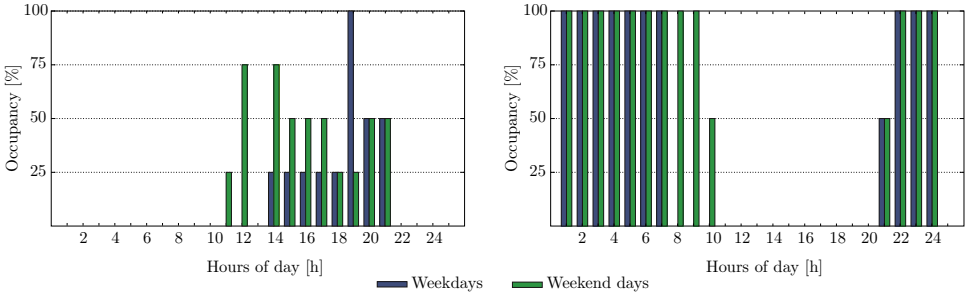

(a) Occupancy of living room **(b)** Occupancy of bedrooms

Fig. 5. Schedules of occupancy for the living room and the bedrooms.

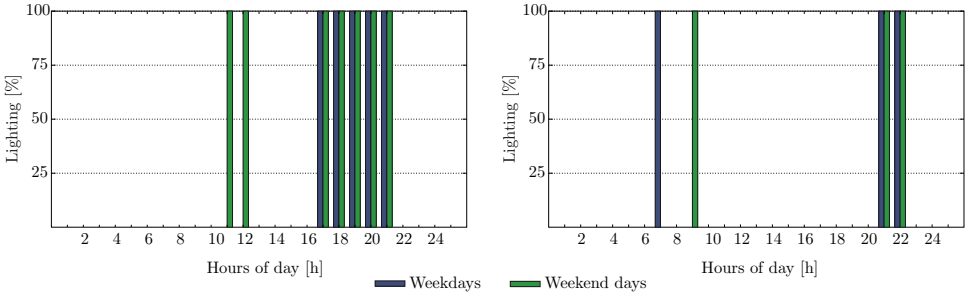

(a) Lighting in living room **(b)** Lighting in bedrooms

Fig. 6. Schedules of lighting for the living room and the bedrooms.

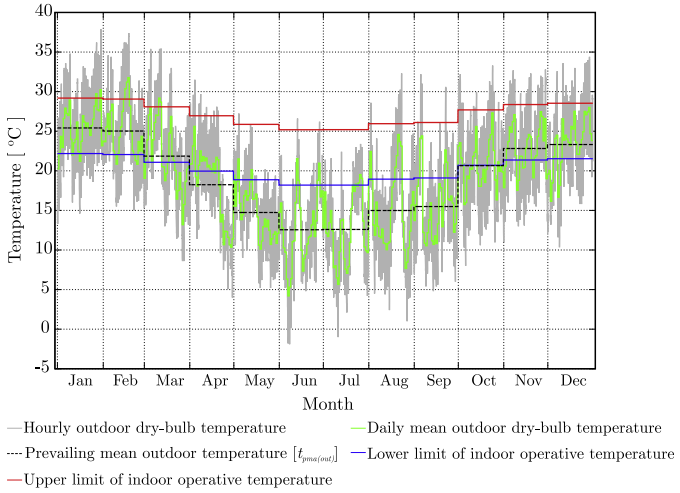

Fig. 7. Mean hourly and daily dry-bulb temperature, prevailing mean outdoor air temperature, and 80% acceptability limits for the city of Paraná.

3.2. Measurement of performance for naturally-ventilated and air-conditioned rooms

Let the degree of thermal discomfort for a naturally-ventilated room be determined by the cooling and heating degree-hours, D_{cool} and D_{heat} respectively, defined as:

$$D_{\text{cool}} = \sum_h \langle T_{\text{op}}(h) - T_{\text{upper}}(h) \rangle, \tag{1}$$

$$D_{\text{heat}} = \sum_h \langle T_{\text{lower}}(h) - T_{\text{op}}(h) \rangle, \tag{2}$$

where $\langle x \rangle$ is the ramp function ($\langle x \rangle$=0 if $x < 0$ and $\langle x \rangle = x$ if $x \geq 0$), $T_{\text{op}}(h)$ is the operative temperature in the room at the hour h (obtained as an output of E$^+$), T_{lower} and T_{upper} are the lower and upper admissible temperature, dependent on local weather conditions; the range of the preceding sums is a whole year, excluding the hours when the room is not occupied. As a unique measure of the discomfort of this room, we used the total degree-hours:

$$D_{\text{total}} = D_{\text{cool}} + D_{\text{heat}}. \tag{3}$$

The admissible temperatures T_{lower} and T_{upper} were defined as the lower and upper 80%-acceptability limits [30]:

$$T_{\text{lower}} = 0.31\, t_{\text{pma(out)}} + 14.3\,^{\circ}\text{C}, \tag{4}$$

$$T_{\text{upper}} = 0.31\, t_{\text{pma(out)}} + 21.3^{\circ}\text{C}, \tag{5}$$

where $t_{\text{pma(out)}}$ is the prevailing mean outdoor temperature, adopted here as the monthly mean of the local dry-bulb temperature, as shown in Fig. 7.

In this work, we have focused on the living-room as the naturally-ventilated room, which was occupied according to the schedule in Fig. 5. On the other hand, for the bedrooms where thermal comfort was artificially enforced if necessary, the thermal performance was rather measured by means of the total annual energy consumption of the air-conditioners:

$$E_{\text{total}} = E_{\text{heat}} + E_{\text{cool}} + E_{\text{fan}}, \tag{6}$$

where E_{heat} and E_{cool} is the energy consumption due by the heat pump and the cooling coil for heating and cooling, respectively, and E_{fan} is the power consumed by the fans during both heating and cooling. All these values are E$^+$ outputs.

3.3. Definition of the global objective function

To improve the performance of the given building implies to minimise the function D_{total} (the thermal discomfort degree-hours in the living room) together with the function E_{total} (the energy consumption of air-conditioners in the bedrooms), which are the so-called objective functions in the context of the Optimisation Theory.

Typically, there are two popular approaches for solving a multi-objective optimisation problem like this [16,31]: the weighted sum approach and the Pareto-based approach. The first one is the classical approach, consisting of defining a unique objective as the weighted sum of the sub-objectives. This single objective can be minimised using typical optimisation algorithms, but you cannot infer how the sub-objectives affect each other, as you can do it using the Pareto-base methods. Cao et al. [32] pointed out that the weighted-sum methods are not only easier to implement but usually more effective and efficient than the Pareto-based methods. Following these authors, the weighted-sum approach was the preferred methodology in this work. Then, we defined a unique, global objective function as

$$f(\mathbf{x}) = w_D \frac{D_{\text{total}}(\mathbf{x})}{D_{\text{total}}(\mathbf{x}_{\text{Dmax}})} + w_E \frac{E_{\text{total}}(\mathbf{x})}{E_{\text{total}}(\mathbf{x}_{\text{Emax}})}, \tag{7}$$

where $\mathbf{x}$ is the set of design variables, w_D and w_E are weighting factors, $\mathbf{x}_{\text{Dmax}}$ and $\mathbf{x}_{\text{Emax}}$ are the set of design variables that maximise D_{total} and E_{total}, respectively; they were determined during the sensitivity analysis in the following section, and are highlighted in Table 2. In this case, motivated by the fact that the periods of occupancy of the living room (involved in D_{total}) and the bedrooms (involved in E_{total}) were similar in extension, we set $w_D = w_E = 0.5$.

4. Sensitivity analysis

The sensitivity analysis serves to determine which of the design (or input) variables have a considerable influence on the objective function (or output). Tian et al. [33] reviewed different methods for sensitivity analysis in building energy modelling. They concluded that the Morris screening method [21] is the best suited for problems with a large number of input variables due to its low computational cost. Following this recommendation, we adopted the Morris method for the sensitivity analysis in this work. Specifically, we used the model implemented into the package "sensitivity" [34] of the free software R for statistical computing [35], including a simplex-based design of experiment [36] as an improvement to the "one-factor-at-a-time" strategy originally used by Morris [21].

For the studied house, we pre-defined $k = 21$ input variables, and each one was allowed to assume four levels as shown in Table 2. For instance, the first design variable is the thermal transmittance of the external walls, which can assume four discrete values (0.75, 1.75, 2.75, and 3.75 W m^{-2} K^{-1}), while the 21st design variable defines the window type, which can be one of the four types described in Table 3.

Morris [21] suggests the use of $k + 1$ points in the input variables space in different r trajectories. For this work, we adopted $r = 20$, so that 20 trajectories or repetitions of the elementary effects were calculated for each input variable. Then, there was $r(k + 1) = 440$ samples.

The Morris method gives two sensitivity indices for each input variable [37]: the mean of the elementary effects, namely μ^*, to measure the effect of this input on the output; and the standard deviation of the elementary effects, namely σ, to assess the strength of the interaction of this input with the other inputs as well as the nonlinearity of the effect of this input on the output. Here, we computed μ^* and σ considering either each sub-objective (total

Table 2
Design variables for thermal performance. The set of design variables $\mathbf{x}_{Dmax}$ making D_{total} maximum are underlined, while the set of design variables $\mathbf{x}_{Emax}$ making E_{total} maximum are in bold.

#	Design variable	ID	Unit	Level 1	Level 2	Level 3	Level 4
1	Thermal transmittance of the external walls	$U_{ExtWall}$	W/m^2 K	0.75	1.75	**2.75**	3.75
2	Thermal transmittance of the internal walls	$U_{IntWall}$	W/m^2 K	0.75	**1.75**	2.75	3.75
3	Thermal transmittance of the first floor	$U_{FirstFloor}$	W/m^2 K	0.8	1.9	3.0	**4.1**
4	Thermal transmittance of the roof	U_{Roof}	W/m^2 K	0.8	**1.9**	3.0	4.1
5	Thermal capacity of the external walls	$C_{ExtWall}$	kJ/m^2 K	**20**	120	220	320
6	Thermal capacity of the internal walls	$C_{IntWall}$	kJ/m^2 K	**20**	120	220	320
7	Thermal capacity the first floor	$C_{FirstFloor}$	kJ/m^2 K	**20**	95	170	245
8	Thermal capacity the roof	C_{Roof}	kJ/m^2 K	**20**	95	170	245
9	Solar absorptance of the external walls	$\alpha_{ExtWall}$	dimensionless	**0.2**	0.4	0.6	0.8
10	Solar absorptance of the roof	α_{Roof}	dimensionless	0.2	**0.4**	0.6	0.8
11	Internal solar absorptance of the floors	α_{Floors}	dimensionless	0.2	**0.4**	0.6	0.8
12	Thermal conductivity of the floor insulation	$K_{InsFloor}$	W/(mK)	**0.04**	0.52	1.01	1.50
13	Thickness of concrete slab of the floors	$T_{SlabFloor}$	m	0.05	**0.10**	0.15	0.20
14	Internal emissivity of the roof	$\varepsilon_{IntRoof}$	dimensionless	0.05	0.35	**0.65**	0.95
15	Windows area fraction	$AF_{Windows}$	dimensionless	1	2	**3**	4
16	Window area fraction for natural ventilation	$AF_{Ventilation}$	dimensionless	0.3	0.5	**0.7**	0.9
17	Doors air infiltration rate	IR_{Doors}	kg/(sm)	10^{-5}	6.67×10^{-3}	$\mathbf{1.33 \times 10^{-2}}$	2.00×10^{-2}
18	Windows air infiltration rate	$IR_{Windows}$	kg/(sm)	10^{-5}	6.67×10^{-3}	$\mathbf{1.33 \times 10^{-2}}$	2.00×10^{-2}
19	Azimuth of the building	β	°	0	90	**180**	270
20	Windows shading	$Sh_{Windows}$	m	0.3	0.6	0.9	**1.2**
21	Windows type	Win_{Type}	-	1	2	3	**4**

Table 3
Window types.

Type	Outside layer	Layer 2	Layer 3
Win-1	Clear 2.5 mm	–	–
Win-2	Clear 6.0 mm	–	–
Win-3	Clear 2.5 mm	Air 10 mm	Clear 2.5 mm
Win-4	Clear 6.0 mm	Air 30 mm	Clear 6.0 mm

degree-hours D_{total} or total energy consumption E_{total}) or the global objective f as output.

4.1. Results from sensitivity analysis

The results of sensitivity analysis in the two bedrooms and the living room, distinguishing cooling and heating, are shown in Fig. 8. Considering energy consumption for cooling and heating, similar patterns were obtained in both bedrooms: Azimuth, solar absorptance and thermal capacity of the external walls, window area fraction for natural ventilation, and thermal capacity of the roof were the most important design variables for cooling (Fig. 8(a) and (c) for bedrooms 1 and 2, respectively), while windows infiltration rate, azimuth, and thermal transmittance of external walls and roof were the most important ones for heating energy consumption (Fig. 8(b) and (d) for bedrooms 1 and 2, respectively).

Regarding cooling degree-hours in the living room, Fig. 8(e) shows that the solar absorptance of external walls was by far the most important design variable; then thermal transmittance and the thermal capacity of externals walls, the windows area fraction for natural ventilation, and the azimuth were the other most relevant variables. In the case of heating degree-hours in the living-room, the most relevant design variable was again the solar absorptance of external walls, and the next four most relevant variables were the same as for cooling (but in a different order), as shown in Fig. 8(f).

Considering cooling and heating together, the influence of the design variables on the total energy consumption at both bedrooms and on the total degree-hours at the living room are shown in Fig. 9(a) and (b), respectively. It can be seen that the windows infiltration rate was by far the most influential variable on total energy consumption in bedrooms, while the thermal transmittance of the external walls was the most relevant one on the total degree-hours at the living room.

Fig. 10 shows the sensitivity of the global objective function to the design variables. All the design variables are ranked considering their effect on the global performance of the house, as measured by the parameter μ^*. We found that some inputs (including the transmittance of the external wall, the infiltration rate in windows, and the orientation of the building) had a considerable impact on the global performance of the house, compared to the effect of the other inputs that could be neglected. A priori, we decided not to keep as design variables all the inputs with $\mu^* < 0.1\mu^*_{max}$ (with $\mu^*_{max} = 0.3216$ corresponding to the thermal transmittance of external walls), remaining in such a way 13 inputs as design variables for the continuation of this work (from the thermal transmittance of external walls to the window area fraction for natural ventilation on the list given in Fig. 10). Later, we decided to keep also the 14th input (windows shading) as design variable since it was expected to be more relevant for the study of a more sophisticated problem (the Case B in Section 5.1 below) where all the surfaces were allowed to be walls of a different kind.

Another interesting conclusion from Figs. 8–10 is how nonlinear the effect of an individual variable is on the sub-objectives or the global objective or how strongly this variable is correlated to the other ones, which is measured by the standard deviation σ [38]. So, in this case, it can be seen from Fig. 10 that azimuth and solar absorptance of external walls were those variables with either the most nonlinear effect on the global objective or the strongest mutual interaction with the other variables, making their effect on the objective the most difficult to predict.

5. Thermal and energy performance optimisation

Improving the performance of the given house implies solving the following mixed integer nonlinear programming (MINLP):

$$\min_{\mathbf{x} \in \mathcal{X}} f(\mathbf{x}), \tag{8}$$

where f, given by Eq. (7), is a global measure of the performance of the house, and $\mathbf{x}$ is the vector of design variables from the feasible design space $\mathcal{X}$. In order to refer the improvement to the original configuration of the house (described in Section 2), let us replace both $\mathbf{x}_{Dmax}$ and $\mathbf{x}_{Emax}$ in Eq. (7) by the set of design variables for the base case (from now on, the Case 0), say $\mathbf{x}_0$, defined in Table 1.

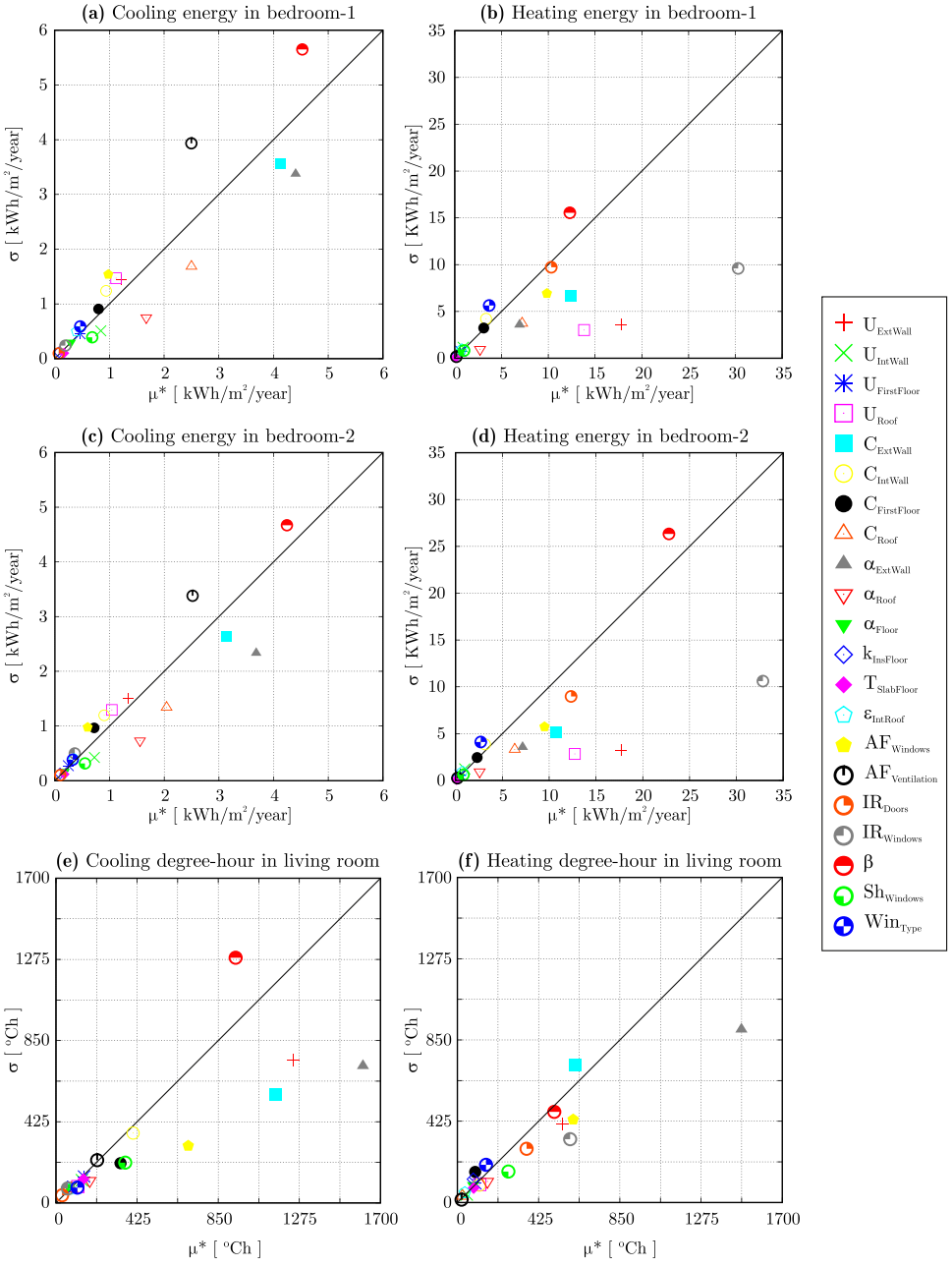

Fig. 8. Mean (μ^*) and standard deviation (σ) of elementary effects for the sub-objectives.

Table 4
Discretization of continuous design variables.

Design variable	Simulation variable	Min. value	Max. value	Step size	Number of cases
Building azimuth [°]	x_1	0	315	45	8
Window shading size [%]	x_2	25	100	25	4
External solar absorptance of the external walls [dimensionless]	x_3	0.3	0.9	0.2	4
Windows infiltration rate [kg/(sm)]	x_4	10^{-5}	2×10^{-2}	6.67×10^{-3}	4
Doors infiltration rate [kg/(sm)]	x_5	10^{-5}	2×10^{-2}	6.67×10^{-3}	4
Window area fraction for natural ventilation [%]	x_6	10	50	10	5
Window width [level][a]	x_7	1	4	1	4

[a] Windows width becomes a categorical variable after discretization.

5.1. Specification of the design variables

As an important result of the previous sensitivity analysis, the design vector **x** does not contain 21 components as originally proposed (see Table 2), but 14, which are those showing the most relevant effect on *f*. Among them, the variables $x_1, x_2, \ldots, x_7$ listed in Table 4 (building azimuth, windows shading size, etc.) are continuous within a certain interval. Further, we decided to group the remainder variables into the categorical variables $x_8, x_9, \ldots, x_{12}$. For instance, the design variables associated with the external walls

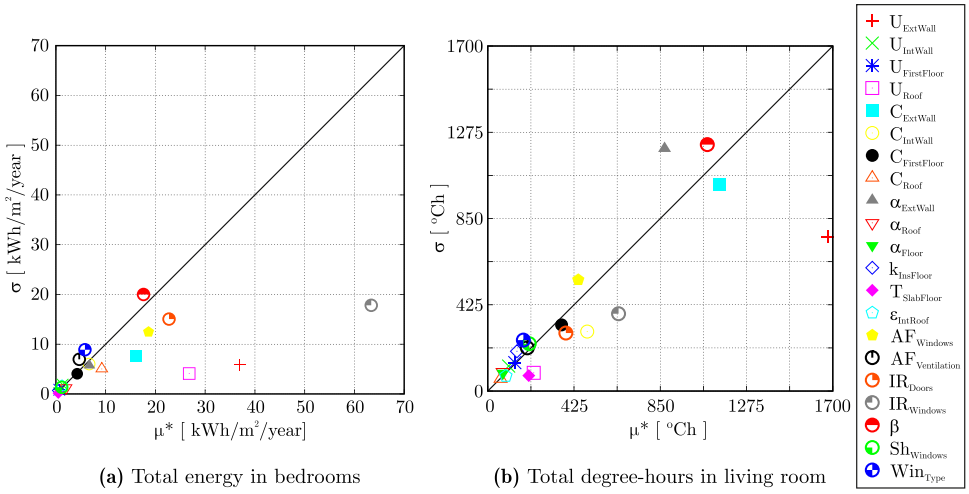

(a) Total energy in bedrooms (b) Total degree-hours in living room

Fig. 9. Mean (μ^*) and standard deviation (σ) of elementary effects for the total energy consumption and total degree-hours.

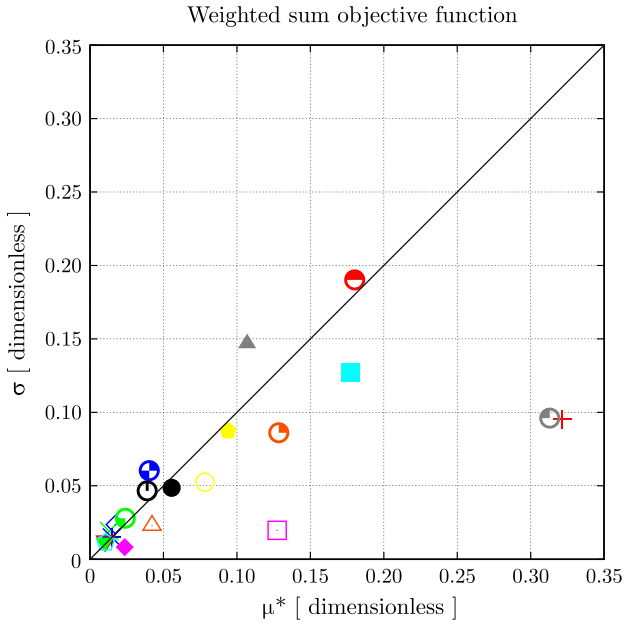

Code	μ*
$U_{ExtWall}$	0.3216
$IR_{Windows}$	0.3130
β	0.1802
$C_{ExtWall}$	0.1771
IR_{Doors}	0.1285
U_{Roof}	0.1274
$\alpha_{ExtWall}$	0.1069
$AF_{Windows}$	0.0940
$C_{IntWall}$	0.0782
$C_{FirstFloor}$	0.0555
C_{Roof}	0.0422
Win_{Type}	0.0403
$AF_{Ventilation}$	0.0389
$Sh_{Windows}$	0.0240
$T_{SlabFloor}$	0.0236
$k_{InsFloor}$	0.0172
$U_{FirstFloor}$	0.0149
$U_{IntWall}$	0.0130
$\varepsilon_{IntRoof}$	0.0107
α_{Roof}	0.0107
α_{Floor}	0.0098

Fig. 10. Mean (μ^*) and standard deviation (σ) of elementary effects for the weighted-sum objective function.

(transmittance and capacity) were grouped in (and replaced by) a unique categorical variable x_8 = Ewall defining the type of external wall. The combination of the different properties of the external walls yielded seven cases (Ewall-1 to Ewall-7 shown in Table 5). The same procedure was applied to the roof, the windows, the internal walls, and the floor of the first floor, giving rise to the categorical variables $x_9, \ldots, x_{12}$, each one replacing the respectively associated group of original variables. All the resulting categorical variables, together with their respective number of predefined cases, are listed in Table 5. The material properties associated with these categorical variables are those defined by the Argentine standard IRAM 11603 for thermal conditioning of buildings [4], shown in Table 6.

While the categorical variables are intrinsically discrete, we decided to discretise the continuous variables, that is, only certain discrete values of them were allowed, mainly to account for constraints of the house building process. For instance, the azimuth β, continuous in the interval [0°, 360°], was allowed to take only eight discrete values (from 0° to 315° every 45°). In order to use the airflow network model in E+ [25], we had to define the "azimuth angle of long axis of building", which is the smaller of the angles between North and the long axis of the building. In this case, it coincides either with β when $\beta \leq 180°$ of with $\beta - 180°$ when $\beta > 180°$. A change in this angle modifies the pressure coefficients on the building façades, which is automatically accounted for by E+ using the surface average calculation method [39] for rectangular buildings (like the studied one). Also, other variables had to be adapted to be taken as inputs by E+: for instance, the window shading size was given in percentage of the height of the corresponding window, and the external solar absorptance was introduced by defining a

Table 5
Categorical design variables.

Design variable	Simulation variable	Description	ID	Number of cases
External walls	x_8	Wood with air gap	Ewall-1	7
		Hollow brickwork layer with mortar finish	Ewall-2	
		Double hollow brickwork layers with insulation and mortar finish	Ewall-3	
		Wood with insulation and plaster finish	Ewall-4	
		Concrete block with cement-plaster finish	Ewall-5	
		Double concrete block with insulation and cement-plaster finish	Ewall-6	
		Concrete	Ewall-7	
Roof type	x_9	Concrete with plaster ceiling	Roof-1	6
		Concrete and hollow ceramic block with plaster ceiling	Roof-2	
		Ceramic tile, air gap and wood liner	Roof-3	
		Ceramic tile, air gap and concrete liner	Roof-4	
		Ceramic tile, air gap, insulation and concrete liner	Roof-5	
		Ceramic tile, air gap, insulation and wood liner	Roof-6	
Window type	x_{10}	Single clear 3 mm thick glass	Win-1	4
		Single clear 6 mm thick glass	Win-2	
		Double clear 3 mm thick glass with air gap	Win-3	
		Double clear 3 mm thick glass with air gap	Win-4	
Internal walls	x_{11}	Wood with air gap	Iwall-1	5
		Hollow brickwork layer with mortar finish	Iwall-2	
		Wood with insulation and plaster finish	Iwall-3	
		Concrete block with cement-plaster finish	Iwall-4	
		Concrete	Iwall-5	
Floor type of the first floor	x_{12}	Concrete with ceramic floor	Floor-1	3
		Concrete with wood floor	Floor-2	
		Insulation, concrete and ceramic floor	Floor-3	

Table 6
Thermal transmittance U, thermal capacity C_t, and thermal delay θ for the different levels of external walls, roof, internal walls, and floor type of the fist floor.

Design parameter	ID	U [W/m^2 K]	C_t [kJ/m^2 K]	θ [h]
External walls	Ewall-1	1.99	64.32	2.75
	Ewall-2	2.09	136.06	3.38
	Ewall-3	0.93	189.34	7.38
	Ewall-4	0.88	59.21	3.65
	Ewall-5	2.78	124.95	3.06
	Ewall-6	0.87	233.30	9.71
	Ewall-7	4.32	240.00	2.40
Roof type	Roof-1	3.68	195.36	2.15
	Roof-2	2.59	90.79	1.53
	Roof-3	2.03	38.91	1.31
	Roof-4	2.06	216.84	4.78
	Roof-5	0.83	217.85	9.08
	Roof-6	0.83	39.92	2.55
Internal walls	Iwall-1	1.99	64.32	2.75
	Iwall-2	2.09	136.06	3.38
	Iwall-3	0.88	59.21	3.65
	Iwall-4	2.78	124.95	3.06
	Iwall-5	4.32	240.00	2.40
Floor type of the first floor	Floor-1	4.71	256.56	2.68
	Floor-2	2.59	213.44	4.36
	Floor-3	0.61	258.59	12.94

zero-mass material with negligible thermal resistance in the outside layer of the external walls.

The window width was allowed to take four levels of increasing magnitude (level 1 for the narrowest, level 4 for the widest) at each windowed façade: 0.70 m, 1.35 m, 2.00 m, 2.70 m for the windows in Surface-1, 0.70 m, 1.60 m, 2.50 m, 3.40 m for the windows in Surface-3, and 0.70 m, 1.40 m, 2.15 m, 2.90 m for the windows in Surface-4. In such a way, the originally continuous design variable x_7 denoting the window width became a categorical variable after discretisation.

Note that the azimuth β was more finely discretised than the other variables. This was a consequence of the previous sensitivity analysis, where we found β to be the variable with highest σ.

At this point, there were 12 discrete design variables, those listed in Tables 4 and 5. Let us call Case A the optimisation problem (8) for these design variables.

Alternatively, in seek of further improvement of the thermal performance, we defined a new optimisation problem, say Case B, having the same objective but more design variables in order to allow each external surface to have its own type of wall, external solar absorptance, window width and window shading size. For instance, the unique variable Ewall defining the type of all the external walls in Case A was replaced by four variables Ewall-Surf1 to Ewall-Surf4 (Surf*i* denoting the corresponding surface *i* in Fig. 4) defining the type of wall of each outer surface. Further, each new variable Ewall-Surf*i* in Case B was allowed to have the same number

of cases as Ewall in Case A. Finally, there were 22 design variables in Case B.

5.2. Selection of optimisation algorithm

Considering the number of possible cases for each one of the variables, there are about 10^8 different designs for Case A, and up to 10^{16} for Case B. Given the huge number of alternatives, it is impossible to simulate all of them in seek of an optimal solution, turning absolutely necessary to use efficient optimisation algorithms.

Several works comparing the performance of different algorithms for building design optimisation problems (BOPs) can be found in the literature. Wetter and Wright [40] compared the Hooke-Jeeves (JS) pattern search method and genetic algorithms (GA) to minimise the building energy consumption. In the light of the test they ran, they concluded that JS convergence was deteriorated by discontinuities in the objective function and was prone to get stuck on local minima, while GA usually arrived at a better minimum. In a later review, Wetter and Wright [41] added several algorithms to the comparison study: the coordinate search algorithm, various versions of particle swarm optimisation (PSO) including a hybrid JS-PSO algorithm, the Nelder-Mead simplex algorithm, and the discrete Armijo gradient algorithm. Based on the results of two numerical experiments on three different cities, they found that the hybrid JS-PSO algorithm usually achieved the best minimum, but was computationally more expensive than GA, whose results were close to the best minimum. Bichiou and Krarti [11] compared GA, PSO and sequential search (SS) in terms of effectiveness and computational cost to optimise the envelope and to select the HVAC system for residential buildings. Showing a similar robustness to arrive at the optimal solution, GA and PSO required considerably less computational time than SS, being GA the fastest method. For the optimisation of the building envelope for residential buildings, Tuhus-Dubrow and Krarti [42] found GA more efficient than PSO and SS when there were more than ten design variables (as in the current case).

Further, Nguyen et al. [15] showed that integer or discrete design variables could produce disorders and discontinuities in the outputs of building performance simulation. This is particularly true for E+, since it uses empirically determined properties (e.g., the wind pressure coefficients) and numerical solution of nonlinear equations. As pointed out by Wetter and Wright [40,41], such discontinuities prevent the use of some optimisation algorithms, like pattern search methods as gradient-based methods.

Therefore, in the light of the above mentioned advantages (efficiency in presence of a large number of design variables, treatment of discontinuities in presence of integer design variables, low computational cost, among others), we decided to use GA to solve the current single-objective optimisation problem.

5.3. Implementation of genetic algorithms

GA is a family of search algorithms based on the evolution of the species by natural selection [43]. The current implementation of GA takes as platform the Distributed Evolutionary Algorithms in Python (DEAP) [44]. To improve the performance of the GA solver in presence of integer design variables, we modified the DEAP Python code to introduce the Laplace crossover and the power mutation techniques, as recommended by Deep et al. [45].

Briefly, the steps for the current GA optimisation process are summarised in the following pseudo-code:

```
population = random(popsize)
Fitness(population)
Update elite list
From 1 to #generations do
  offspring = Selection(population)
  offspring = Crossover(offspring)
  offspring = Mutation(offspring)
  Fitness(offspring)
  Update elite list
  population = offspring
End
```

This is basically the structure of DEAP. During each fitness step, the objective $f(\mathbf{x})$ is calculated for each individual $\mathbf{x}$ in the population. To this end, we wrote a Python routine that takes each $\mathbf{x}$ from the GA solver as input arguments, converts the entries of $\mathbf{x}$ in E+ inputs, writes the corresponding E+ input file (.idf), calls E+ to run this file, reads the E+ output file (.csv) to determine the operative temperature in the living room and the energy consumed by the air-conditioners in the bedrooms, and finally computes $f(\mathbf{x})$.

The GA settings (population size, selection, crossover and mutation methods, the probability of mutation and crossover, etc.) depend on the characteristics of the optimisation problem [46]. Normally, the population size ranges from 5 to 100%, probability of crossover ranges from 70 to 100%, and the probability of mutation ranges from 0.1% to 5% for building design optimisation [40,41]. In our case, the best results were found for the GA configuration shown in Table 7.

Table 7
Settings of genetic algorithms for the cases analysed.

	Case A	Case B
Population size	30	100
Number of generations	100	100
Elite individuals	1	1
Selection	Tournament	
Crossover method	Laplace crossover	
Crossover probability	95%	95%
Mutation method	Power mutation	
Mutation probability	5%	5%

5.4. Results from optimisation analysis

Fig. 11 gives a general insight into the convergence of GA for the current problems. For Case A, Fig. 11 (a) shows the evolution of the global objective function f for the best individual and the mean of f for all the individuals of the population from generation to generation. It can be seen that f was drastically reduced (i.e., the performance was considerably improved) after a few generations (after 6 generations, f decreased from 1 to 0.112). After that, the convergence was slower until attaining the best value $f_{best,A} = 0.102$ at the 100th generation. A similar conclusion arose by observing the difference between the best and the mean f, which was very small after a few generations.

Fig. 11 (b) shows the evolution of the best and the mean f for Case B. The convergence for Case B was worse than for Case A, since sensible falls of f were observed even at the 73th generation. Actually, the best f for Case B was not smaller than the best f for the simpler Case A before the 74th generation. The best f for case B was $f_{best,B} = 0.088$ at the 100th generation.

Fig. 11(c) and (d) show the evolution of the degree-hours in the living room for Cases A and B, respectively. For both cases, the decrease of the total degree-hours usually accompanied the decrease of the global f, except for the last generations, where the total-degree hours for heating sensibly increased and became larger than the degree-hours for cooling.

Fig. 11(e) and (f) show the evolution of the energy consumption in the bedrooms for Cases A and B, respectively. Note that cooling was always the dominant source of energy consumption in the bedrooms.

Table 8 shows the optimal configurations for both cases. For some design variables the optimal solutions for Case A were very different from those for Case B: Surface-1 was optimally oriented

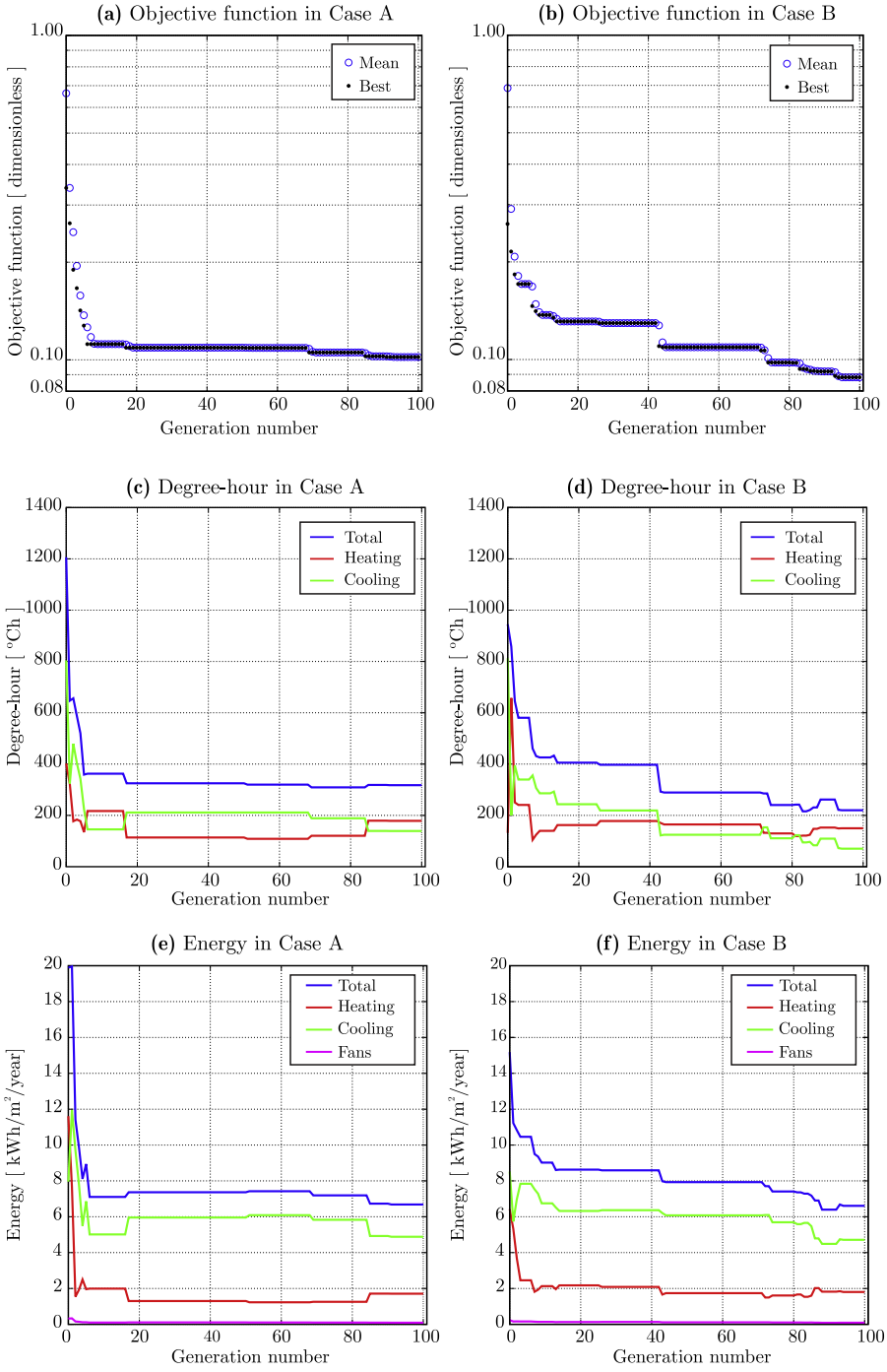

Fig. 11. Convergence of the optimisation objectives.

when it faced West for Case A, and North for Case B. The optimal windows width for Case A was a compromise solution (level 2 of 4); for Case B, the optimal windows width was the maximal one (level 4) in the North-facing surface, the minimal one (level 1) in the South-facing surface, and an intermediate one (level 2) in the East-facing surface. All the optimal windows were completely shaded for Case A; only the windows facing West were completely shaded while the others were minimally shaded for Case B. The optimal windows area fraction for natural ventilation coincided with the prescribed lower bound (10% of the windows area) for Case A, while it reached the prescribed upper bound (50% of the windows area) for Case B. Also for the doors infiltration rate, the optimal value coincided either with the lower or the upper prescribed bound for Cases A and B, respectively. For the external thermal absorptance, a compromise solution (0.5) was adopted as optimal for Case A, while the optimal was found to be 0.9 (upper bound) for the North-facing surface, 0.5 for the South-facing surface, and 0.3 (lower bound) for the East- and West-facing surfaces.

Regarding the optimal choice of external walls type, Ewall-6 was found to be the optimal for Case A, and for the surfaces facing South, East and West in Case B; the optimal North-facing surface for Case B was found to be Ewall-3. Let us note that Ewall-3 and Ewall-6 are physically similar, both having low thermal transmittance, high thermal capacity and high delay, as seen in Table 6.

Besides the similar choice of external walls, both cases were coincident at their corresponding optimal configuration in the

Table 8
Results of the optimal configurations for the design variables.

Design variable	Surface	Case A	Case B
Building azimuth [degree]	–	270	0
Window shading size [%]	Surface-1	100	25
	Surface-2		–
	Surface-3		25
	Surface-4		100
External solar absorptance of the external walls [dimensionless]	Surface-1	0.5	0.9
	Surface-2		0.5
	Surface-3		0.3
	Surface-4		0.3
Window width [level]	Surface-1	2	4
	Surface-2		–
	Surface-3		1
	Surface-4		2
Windows infiltration rate [kg/(sm)]	–	10^{-5}	10^{-5}
Doors infiltration rate [kg/(sm)]	–	10^{-5}	2×10^{-2}
Window area fraction for natural ventilation [%]	–	10	50
External walls	Surface-1	Ewall-6	Ewall-3
	Surface-2		Ewall-6
	Surface-3		Ewall-6
	Surface-4		Ewall-6
Roof type	–	Roof-5	Roof-5
Window type	–	Win-4	Win-4
Internal walls	–	Iwall-5	Iwall-5
Floor type of the first floor	–	Floor-3	Floor-3

Table 9
Thermal and energy performance for Cases 0 (base), A and B (optimal).

Objective and sub-objectives	Thermal and energy performance				Relative improvements		
	Units	Case 0	Case A	Case B	Case A/Case 0	Case B/Case 0	Case B/Case A
Global objective	–	1.000	0.102	0.088	0.102	0.088	0.863
Total degree-hour	°Ch	3690.190	317.748	220.169	0.086	0.060	0.693
Heating degree-hour	°Ch	1454.410	178.704	149.897	0.123	0.103	0.839
Cooling degree-hour	°Ch	2235.780	139.044	70.274	0.062	0.031	0.505
Total energy consumption	kWh/m^2/year	56.720	6.684	6.612	0.118	0.117	0.989
Heating energy consumption	kWh/m^2/year	44.390	1.708	1.806	0.038	0.041	1.057
Cooling energy consumption	kWh/m^2/year	11.570	4.883	4.714	0.422	0.407	0.965
Fans energy consumption	kWh/m^2/year	0.750	0.092	0.091	0.123	0.121	0.989

choice of windows infiltration rate (10^{-5} kg/(sm), that was the lower bound), the types of roof (Roof-5, the one with the lowest transmittance and the highest thermal capacity and delay in Table 6), internal walls (Iwall-5, that with the highest thermal transmittance and capacity and the lowest delay in Table 6), floor of the first floor (Floor-3, having the lowest transmittance and the highest thermal capacity and delay in Table 6) and windows glassing (Win-4, the one having the lowest transmittance). General recommendations for building this type of house in Littoral can be derived from these common results for Cases A and B.

The results for Case B were clearly sensitive to the local weather: Solar gains were favoured through the North-facing façade (large and little shaded windows and high external thermal absorptance) while they were controlled through East- and West-facing façades (not very large and well shaded windows and low external solar absorptance). Given the large number of inter-related design variables and their usually nonlinear effect on the objective, such conclusions could only be envisaged after the solution of an optimisation problem.

Optimisation results are summarised in Table 9, highlighting the improvements obtained with respect to the original design (Case 0). The total degree-hours in the naturally ventilated living room decreased from $D_{\text{total}}(\mathbf{x}_0) = 3690$°Ch for Case 0 to $D_{total}(\mathbf{x}_\mathbf{A}^{\mathbf{opt}}) = 0.086 D_{total}(\mathbf{x_0})$ and $D_{total}(\mathbf{x}_\mathbf{B}^{\mathbf{opt}}) = 0.060 D_{total}(\mathbf{x_0})$ for the optimal solutions $\mathbf{x}_\text{A}^{\text{opt}}$ and $\mathbf{x}_\text{B}^{\text{opt}}$ of Cases A and B, respectively. Further, the solution of Case B was considerably better than the solution of Case A in terms of D_{total}: $D_{total}(\mathbf{x}_\mathbf{B}^{\mathbf{opt}}) = 0.693 D_{total}(\mathbf{x}_\mathbf{A}^{\mathbf{opt}})$. It is particularly remarkable the solution of Case B considering the reduction of the degree-hours for cooling: $D_{cool}(\mathbf{x}_\mathbf{B}^{\mathbf{opt}}) = 0.505 D_{cool}(\mathbf{x}_\mathbf{A}^{\mathbf{opt}}) = 0.031 D_{cool}(\mathbf{x_0})$.

The energy consumption for air-conditioning in the bedrooms was reduced from $E_{\text{total}}(\mathbf{x}_0) = 56.72$ kWh/m^2/ year to $E_{\text{total}}(\mathbf{x}_\text{A}^{\text{opt}}) = 0.118 E_{\text{total}}(\mathbf{x}_0)$ and $E_{\text{total}}(\mathbf{x}_\text{B}^{\text{opt}}) = 0.117 E_{\text{total}}(\mathbf{x}_0)$. Here, the solution of the more sophisticated Case B did not produce a sensible improvement of E_{total} compared to the solution of the simpler Case A.

The global objective decreased from $f(\mathbf{x}_0) = 1$ to $f(\mathbf{x}_\text{A}^{\text{opt}}) = 0.102$ and $f(\mathbf{x}_\text{B}^{\text{opt}}) = 0.088$. Note that this decrease in the global weighted-sum function f was accompanied by decreases of the same order in both sub-objectives D_{total} and E_{total}. This indicates, first, that both sub-objectives are not contradictory, and, second, that the weights assigned to the sub-objectives were correct, validating our choice of the weighted-sum approach. A final argument for the effectiveness of this simple approach for the current application is the impressive reduction in D_{total} and E_{total} for the optimal designs compared to the original Case 0, which is a real, typical house as it is built today in Littoral: D_{total} and E_{total} are reduced up to 91% and 88%, respectively.

Regarding the computational cost, the solution of Cases A and B took respectively 3000 and 10000 fitness evaluations (=population size×number of generations), which is negligible compared to the

size of the whole search space (10^8 for Case A and 10^{16} for Case B). Then, the weighted-sum approach proved to be not only effective but computationally efficient for the current application.

6. Conclusions

In this work, we optimised the thermal and energy performance of a typical single-family house in the Argentine Littoral region using simulation-based optimisation. The performance of the house was characterised by a unique, global objective function defined as the weighted-sum of two sub-objectives: the total degree-hours in the living room and the energy consumption for air-conditioning in the bedrooms. A set of design variables was defined, and the sensitivity of the global objective and the sub-objectives to these design variables was analysed using the Morris screening method. By this way, we detected the more relevant design variables and only them were involved in the optimisation problem.

As result of the optimisation, we achieved impressive reductions not only in the global objective but also in the sub-objectives: up to 91% fewer total degree-hours in the living room and up to 88% less energy consumption in the bedrooms (up to 91% and 88%, respectively) compared to the original design (that of a typical single-family house in Littoral as it is being currently built). This validated the use of the simple weighted-sum approach for solving the current multi-objective optimisation problem.

Further, results served to dictate some general recommendations for the design of such typical houses in Littoral, including: External walls and roofs should have low thermal transmittance and high thermal capacity and high thermal delay, while the internal ones should have high thermal transmittance and capacitance and low delay; and the windows should have low transmittance.

As future work, other building typologies and sub-objectives will be considered. These sub-objectives should account for the life-cycle cost, the environmental impacts, and architectural and technological constraints. We expect that, for such a diverse simultaneous objectives, the use of more sophisticated multi-objective algorithms (the Pareto-based ones) will be mandatory, becoming a next research interest.

Acknowledgements

For funding this work, we would like to thank the following institutions:

1. Secretary for Science, Technology and Innovation (SECTEI) of the Province of Santa Fe, Argentina, via the project 2010-040-13 Res. SECTEI 117/13.
2. Universidad Nacional del Litoral (UNL), Argentina, via the project CAI+D 2011 50120110100441LI.

This work was partially done during the three-month internship of F. Bre at the Laboratory of Energy Efficiency in Buildings, Federal University of Santa Catarina (Brazil), thanks to a scholarship given by the Association of Universities Montevideo Group (AUGM).

F. Bre is a doctoral student granted by the National Scientific and Technical Research Council of Argentina (CONICET).

References

[1] Ministerio de Energía y Minería de la República Argentina [Argentine Ministry of Energy and Mining]. Balance energético nacional – Año 2014 – Revisión B [National energy balance – Year 2014 – Revision B] (in Spanish), 2014. http://www.energia.gov.ar/contenidos/verpagina.php?idpagina=3366.

[2] Boletín Oficial de la República Argentina [Argentine Official Gazzette]. Decreto 134/2015: Emergencia energética [Decrete 134/2015: Energy emergency] (in Spanish), December 17th, 2015. https://www.boletinoficial.gob.ar/pdf/linkQR/Nnh0S05RRXhTRFUrdTVReEh2ZkU0dz09.

[3] M.C. Peel, B.L. Finlayson, T.A. McMahon, Updated world map of the Köppen-Geiger climate classification, Hydrol. Earth Syst. Sci. 11 (2007) 1633–1644.

[4] Instituto Argentino de Normalización y Certificación [Argentine Institute of Standards and Certification] (IRAM). IRAM 11603. Acondicionamiento térmico de edificios. Clasificación bioambiental de la República Argentina [Thermal conditioning of buildings. Bioenvironmental classification of Argentina] (in Spanish), 2012.

[5] Intergovernmental Panel on Climate Change (IPCC), Climate Change 2014: Impacts, Adaptation, and Vulnerability. Part B: Regional Aspects. Contribution of Working Group II to the Fifth Assessment Report of the Intergovernmental Panel on Climate Change, Cambridge University Press, 2014.

[6] M.J. Scott, Y.J. Huang, Effects of climate change on energy use in the United States, in: Effects of Climate Change on Energy Production and Use in the United States. A Report by the U.S. Climate Change Science Program and the Subcommittee on Global Change Research, 2007, Washington, DC, Chapter 2.

[7] R. Garber, Optimisation stories: the impact of building information modelling on contemporary design practice, Architect. Des. 79 (2) (2009) 6–13.

[8] D.B. Crawley, L.K. Lawrie, F.C. Winkelmann, W.F. Buhl, Y.J. Huang, C.O. Pedersen, R.K. Strand, R.J. Liesen, D.E. Fisher, M.J. Witte, J. Glazer, EnergyPlus: creating a new-generation building energy simulation program, Energy Build. 33 (4) (2001) 319–331.

[9] J.A. Wright, The optimised design of HVAC systems (Ph.D. thesis), Loughborough University of Technology, Leicestershire, UK, 1986.

[10] M. Fesanghary, S. Asadi, Z.W. Geem, Design of low-emission and energy-efficient residential buildings using a multi-objective optimization algorithm, Build. Environ. 49 (2012) 245–250.

[11] Y. Bichiou, M. Krarti, Optimization of envelope and HVAC systems selection for residential buildings, Energy Build. 43 (12) (2011) 3373–3382.

[12] P. Ihm, M. Krarti, Design optimization of energy efficient residential buildings in tunisia, Build. Environ. 58 (2012) 81–90.

[13] A.-T. Nguyen, S. Reiter, Passive designs and strategies for low-cost housing using simulation-based optimization and different thermal comfort criteria, J. Build. Perform. Simul. 7 (1) (2014) 68–81.

[14] R. Evins, A review of computational optimisation methods applied to sustainable building design, Renew. Sustain. Energy Rev. 22 (2013) 230–245.

[15] A.-T. Nguyen, S. Reiter, P. Rigo, A review on simulation-based optimization methods applied to building performance analysis, Appl. Energy 113 (2014) 1043–1058.

[16] V. Machairas, A. Tsangrassoulis, K. Axarli, Algorithms for optimization of building design: a review, Renew. Sustain. Energy Rev. 31 (2014) 101–112.

[17] H. Ren, W. Gao, Y. Ruan, Economic optimization and sensitivity analysis of photovoltaic system in residential buildings, Renew. Energy 34 (3) (2009) 883–889.

[18] P. Heiselberg, H. Brohus, A. Hesselholt, H. Rasmussen, E. Seinre, S. Thomas, Application of sensitivity analysis in design of sustainable buildings, Renew. Energy 34 (9) (2009) 2030–2036.

[19] A.S. Silva, L.S.S. Almeida, E. Ghisi, Decision-making process for improving thermal and energy performance of residential buildings: a case study of constructive systems in Brazil, Energy Build. 128 (2016) 270–286.

[20] R. Evins, P. Pointer, R. Vaidyanathan, S. Burgess, A case study exploring regulated energy use in domestic buildings using design-of-experiments and multi-objective optimisation, Build. Environ. 54 (2012) 126–136.

[21] M.D. Morris, Factorial sampling plans for preliminary computational experiments, Technometrics 33 (2) (1991) 161–174.

[22] F. Bre, V.D. Fachinotti, Generation of typical meteorological years for the Argentine Littoral region, Energy Build. 129 (2016) 432–444.

[23] Administración Nacional de la Seguridad Social de la República Argentina [Argentine Social Security Administration] (ANSES). Programa de Crédito Argentino [Argentine Loans Programme] (PROCREAR) (in Spanish), 2016. http://www.procrear.anses.gob.ar/.

[24] Simulation Research Group at Lawrence Berkeley National Laboratory, Building Systems Laboratory at University of Illinois Urbana-Champaign, et al., EnergyPlus™ Documentation, v8.4.0 – Engineering Reference, 2015 https://energyplus.net/documentation.

[25] U.S. Department of Energy (DoE), EnergyPlus, Input Output Reference – The Encyclopedic Reference to EnergyPlus Input and Output, 2012.

[26] S. Andolsun, C.H. Culp, J.S. Haberl, M.J. Witte, EnergyPlus vs DOE-2. 1e: the effect of ground coupling on cooling/heating energy requirements of slab-on-grade code houses in four climates of the US, Energy Build. 52 (2012) 189–206.

[27] L. Xing, Estimations of Undisturbed Ground Temperatures Using Numerical and Analytical Modeling (Ph.D. thesis), Oklahoma State University, 2014.

[28] Instituto Nacional de Metrologia, Normalizaç ao e Qualidade Industrial [Brazilian Institute of Metrology, Standards and Industrial Quality] (INMETRO). Regulamento técnico da qualidade para o nível de eficiência energética de edificaçoes residenciais [Technical regulation of quality for the energy efficiency level of residential buildings] (RTQ-R) (in Portuguese), 2012.

[29] American Society of Heating, Refrigerating and Air-Conditioning Engineers (ASHRAE), 2009 ASHRAE® Handbook – Fundamentals. Atlanta, Georgia, USA, 2009.

[30] American National Standards Institute (ANSI), American Society of Heating, Refrigerating and Air-Conditioning Engineers (ASHRAE), ANSI/ASHRAE

Standard 55-2013. Thermal Environmental Conditions for Human Occupancy, 2013.
[31] A. Konak, D.W. Coit, A.E. Smith, Multi-objective optimization using genetic algorithms: a tutorial, Reliab. Eng. Syst. Saf. 91 (9) (2006) 992–1007.
[32] K. Cao, B. Huang, S. Wang, H. Lin, Sustainable land use optimization using boundary-based fast genetic algorithm, Comput. Environ. Urban Syst. 36 (2012) 257–269.
[33] W. Tian, A review of sensitivity analysis methods in building energy analysis, Renew. Sustain. Energy Rev. 20 (2013) 411–419.
[34] G. Pujol, B. Iooss, A. Janon, R Package for Sensitivity Analysis, 2015.
[35] R. R Core Team, A Language and Environment for Statistical Computing, R Foundation for Statistical Computing, Vienna, Austria, 2016 http://www.R-project.org.
[36] G. Pujol, Simplex-based screening designs for estimating metamodels, Reliab. Eng. Syst. Saf. 94 (2009) 1156–1160.
[37] A. Saltelli, S. Tarantola, F. Campolongo, M. Ratto, Sensitivity Analysis in Practice: A Guide to Assessing Scientific Models, John Wiley & Sons, 2004.
[38] D. Garcia Sanchez, B. Lacarrière, M. Musy, B. Bourges, Application of sensitivity analysis in building energy simulations: combining first- and second-order elementary effects methods, Energy Build. 68 (2014) 741–750.
[39] M.V. Swami, S. Chandra, Correlations for pressure distribution on buildings and calculation of natural-ventilation airflow, ASHRAE Trans. 94 (3112) (1988) 243–266.
[40] M. Wetter, J. Wright, Comparison of a generalized pattern search and a genetic algorithm optimization method, in: Proceedings of the 8th International IBPSA Conference, Eindhoven, Netherlands, 2003, pp. 1401–1408.
[41] M. Wetter, J. Wright, A comparison of deterministic and probabilistic optimization algorithms for nonsmooth simulation-based optimization, Build. Environ. 39 (8) (2004) 989–999.
[42] D. Tuhus-Dubrow, M. Krarti, Genetic-algorithm based approach to optimize building envelope design for residential buildings, Build. Environ. 45 (7) (2010) 1574–1581.
[43] D.E. Goldberg, J.H. Holland, Genetic algorithms and machine learning, Mach. Learn. 3 (2) (1988) 95–99.
[44] F.-A. Fortin, F.-M. De Rainville, M.-A. Gardner, M. Parizeau, DEAP: evolutionary algorithms made easy, J. Mach. Learn. Res. 13 (July) (2012) 2171–2175.
[45] K. Deep, K.P. Singh, M.L. Kansal, C. Mohan, A real coded genetic algorithm for solving integer and mixed integer optimization problems, Appl. Math. Comput. 212 (2) (2009) 505–518.
[46] K. Deb, Multi-objective Optimization Using Evolutionary Algorithms, vol. 16, John Wiley & Sons, 2001.